

# Non-specific phospholipase C1 affects silicon distribution and mechanical strength in stem nodes of rice

Huasheng Cao<sup>1</sup>, Lin Zhuo<sup>1</sup>, Yuan Su<sup>2</sup>, Linxiao Sun<sup>1</sup> and Xuemin Wang<sup>2,3,\*</sup>

<sup>1</sup>National Key Laboratory of Crop Genetic Improvement, Huazhong Agricultural University, Wuhan 430070, China,

<sup>2</sup>Department of Biology, University of Missouri, St. Louis, Missouri 63121, USA, and

<sup>3</sup>Donald Danforth Plant Science Center, St. Louis, Missouri 63132, USA

Received 26 May 2015; revised 3 March 2016; accepted 7 March 2016; published online 16 March 2016.

\*For correspondence (e-mail swang@danforthcenter.org).

## SUMMARY

**Silicon, the second abundant element in the crust, is beneficial for plant growth, mechanical strength, and stress responses. Here we show that manipulation of the non-specific phospholipase C1, NPC1, alters silicon content in nodes and husks of rice (*Oryza sativa*). Silicon content in NPC1-overexpressing (OE) plants was decreased in nodes but increased in husks compared to wild-type, whereas RNAi suppression of NPC1 resulted in the opposite changes to those of NPC1-OE plants. NPC1 from rice hydrolyzed phospholipids and galactolipids to generate diacylglycerol that can be phosphorylated to phosphatidic acid. Phosphatidic acid interacts with Lsi6, a silicon transporter that is expressed at the highest level in nodes. In addition, the node cells of NPC1-OE plants have lower contents of cellulose and hemicellulose, and thinner sclerenchyma and vascular bundle fibre cells than wild-type plants; whereas NPC1-RNAi plants displayed the opposite changes. These data indicate that NPC1 modulates silicon distribution and secondary cell wall deposition in nodes and grains, affecting mechanical strength and seed shattering.**

**Keywords:** non-specific phospholipase C, phosphatidic acid, silicon distribution, secondary cell wall, seed shattering.

## INTRODUCTION

Membrane lipids are essential to cellular structures and metabolism, and are also important sources for generating mediators regulating various cellular processes. Phospholipase-catalyzed lipid hydrolysis often constitutes an early step in generating lipid mediators, such as diacylglycerol (DAG) and phosphatidic acid (PA). Phosphoinositide-hydrolyzing phospholipase C (PI-PLC) that produces DAG and inositol-phosphates has been studied in-depth in animal cells for the function in cell signalling, cytoskeletal dynamics, vesicular trafficking, and secretion (Kadamur and Ross, 2013). PI-PLCs in mammalian cells are comprised of multiple types (PLC $\beta$ ,  $\gamma$ ,  $\delta$ ,  $\epsilon$ ,  $\zeta$ ,  $\eta$ ). The domain structure of PI-PLCs in plants shows a certain similarity towards the simplest mammalian PI-PLC, PLC $\zeta$  (Wang, 2004; Pokotylo *et al.*, 2014). Conversely, studies in recent years have indicated that higher plants have another family of intracellular PLC, referred to as non-specific PLC (NPC). NPCs share sequence similarity with PC-PLCs in Gram-negative bacteria, and are distinctively different from PI-PLCs (Nakamura *et al.*, 2005; Peters *et al.*, 2010; Pokotylo *et al.*, 2013).

The NPC family is composed of multiple members, and the Arabidopsis genome has six NPCs. The analyses of NPCs in Arabidopsis indicate that NPCs play important and diverse roles in various processes, such as response to phosphate (Pi) deficiency, salt stress, aluminium toxicity, abscisic acid, and brassinosteroid (Gaude *et al.*, 2008; Pejchar *et al.*, 2010; Peters *et al.*, 2010, 2014; Wimalasekera *et al.*, 2010; Kocourkova *et al.*, 2011). NPC5 is involved in membrane glycerolipid remodelling, promoting PC hydrolysis and digalactosyldiacylglycerol (DGDG) accumulation in leaves under phosphorus deprivation (Gaude *et al.*, 2008). A recent study indicated that NPC5 and its lipid product DAG promote lateral root growth and pattern formation under salt stress (Peters *et al.*, 2014). NPC4 plays important roles in response to hormone and different abiotic stress, such as abscisic acid and hyperosmotic stress (Peters *et al.*, 2010), phosphorus deprivation in roots (Nakamura *et al.*, 2005; Gaude *et al.*, 2008), and aluminium toxicity (Pejchar *et al.*, 2015). It has been proposed that under a well watered condition NPC4-derived DAG promotes stomata opening, while under hyperosmotic stress

DAG is converted to PA that modulates stomatal closure and root growth (Peters *et al.*, 2010). NPC3 and NPC4 have been implicated to function in brassinosteroid response and root growth (Wimalasekera *et al.*, 2010). In terms of gene structure and amino acid sequences, NPC3, NPC4, and NPC5 are more closely related to each other than to other NPCs. A recent study indicated that NPC1 positively mediates Arabidopsis response to heat stress (Krčková *et al.*, 2015).

To investigate the function of NPCs in crop and monocot species, we analyzed the function of NPC1 in rice and found that altered expression of *NPC1* affected the mechanical strength and silicon (Si) distributions in nodes and husks. Silicon is a main component of secondary cell walls (Epstein and Bloom, 2005). Here we use under- and over-expression of *NPC1* to show that NPC1 impacts lipid levels, cellulose content, silicon distribution, mechanical strength of rice nodes, and seed shattering; genetic alterations of *NPC1* thus have consequences for rice production.

## RESULTS

### The rice NPC family and expression pattern

NPCs have three conserved motifs that are not related to any other known plant phospholipases, the ENRSFDHxxxG motif at the beginning of the phosphoesterase domain and the TxPNR and YDExGGxxDHV motifs of the phosphoesterase domain (Figure S1a). The rice genome has five NPC genes that are designated as *OsNPC1*, 2, 3, 4, 6, on the basis of gene structures and sequence similarities to Arabidopsis NPCs. NPCs from rice and Arabidopsis can be grouped into four clusters, I (*OsNPC1*, *AtNPC1*), II (*OsNPC2*, *AtNPC2*), III (*OsNPC3*, *OsNPC4*, *AtNPC3*, *AtNPC4*, *AtNPC5*) and IV (*OsNPC6*, *NPC6*) (Figure S1b and Table S1). The length of NPC proteins is similar, about 350 amino acids. Proteins with sequence similarity to *OsNPC1* were identified in some plant species examined, including *Glycine max* (eudicots), *Sorghum bicolor* (monocots), *Selaginella moellendorffii* (lycophytes), and *Physcomitrella paten* (mosses) (Tables S1 and S2 and Figure S1b).

The transcript levels of rice NPCs in tissues were determined by quantitative reverse transcription polymerase chain reaction (RT-PCR) (Figure 1a). *NPC1* did not display strong differential expression in tissues as did other NPCs. The transcript of *NPC1* was present in all tissues examined, including roots, seedlings, leaf blades, leaf sheathes of rice at the 4-leaf stage, nodes, internodes, and panicles at the flowering stage, as well as callus. In comparison, the transcript levels of *NPC3* and *NPC6* were highest in panicles whereas those of *NPC2* and *NPC4* were highest in roots. The tissue patterns of NPCs transcript levels were comparable with those in the database RiceXPro (<http://ricexpro.dna.affrc.go.jp/>; Figure S2a).

*NPC1* does not contain signal sequences indicative of its subcellular localization. When proteins from NPC1: FLAG transgenic rice leaves was fractionated into cytosolic and microsomal fractions, *NPC1* was detected in both the soluble and membrane-associated fractions (Figure S2b). Microsomal membranes were fractionated into the plasma membrane and intracellular membrane fractions by two-phase-partitioning. Marker enzymes activity assay indicated that the plasma and intracellular membrane fractions were enriched in the respective membranes (Figure S2b). The activity of vanadate-sensitive ATPase was higher in the plasma membrane fraction whereas the activity of Cyt c reductase and oxidase, marker enzymes of ER and mitochondria, respectively, was higher in the intracellular membranes than the plasma membrane. *NPC1* protein was found in the plasma and intracellular membranes with most being associated with the intracellular membranous fraction (Figure S2c). Subcellular localization using NPC1: GFP fusion indicated that NPC1 in Arabidopsis is mostly associated with the intracellular membranes (Krčková *et al.*, 2015).

### Overexpression of *OsNPC1* results in brittle nodes and seed shattering

To explore the function of NPC in rice, we focused on NPC1 because information on cluster I NPCs was limited and *NPC1* was expressed in all tissues highly relative to other NPCs (Figure 1a). Transgenic lines that overexpressed *NPC1* (*NPC1*-OE) were generated and positive transgenic OE plants were confirmed by immunoblotting with the antibody against the FLAG tag fused to the C-terminus of NPC1 (Figure 1b). In addition, multiple *NPC1*-RNAi lines of rice were generated to suppress its expression (Figure 1c). The transcript level of *NPC1* in *NPC1*-OE plants was about 15 times greater than in wild-type (WT) whereas that in RNAi plants was decreased by 70% (Figure 1d).

*NPC1*-OE and RNAi plants were morphologically indistinguishable from WT. However, we noticed that during handling, *NPC1*-OE had brittle stem nodes that were snapped easily by bending (Figure 2a). The breaking force for *NPC1*-OE nodes was less than one-fifth of that required for WT whereas that for *NPC1*-RNAi was about one-tenth greater than WT (Figure 2b). In addition, the brittle phenotype was also observed in panicle nodes of *NPC1*-OE (Figure 2c). The mature seeds of *NPC1*-OE rice were easily threshed off the head, increasing seed shattering (Figure 2d).

### *OsNPC1* decreases cell wall deposition in nodes

To gain insights into the cause of the brittle nodes, we examined cell wall morphology of the nodes and internodes. Sclerenchyma cells and vascular bundles in the two tissues provide mechanical support for the plant body (Zhou *et al.*, 2009). When comparing to WT, the thickness

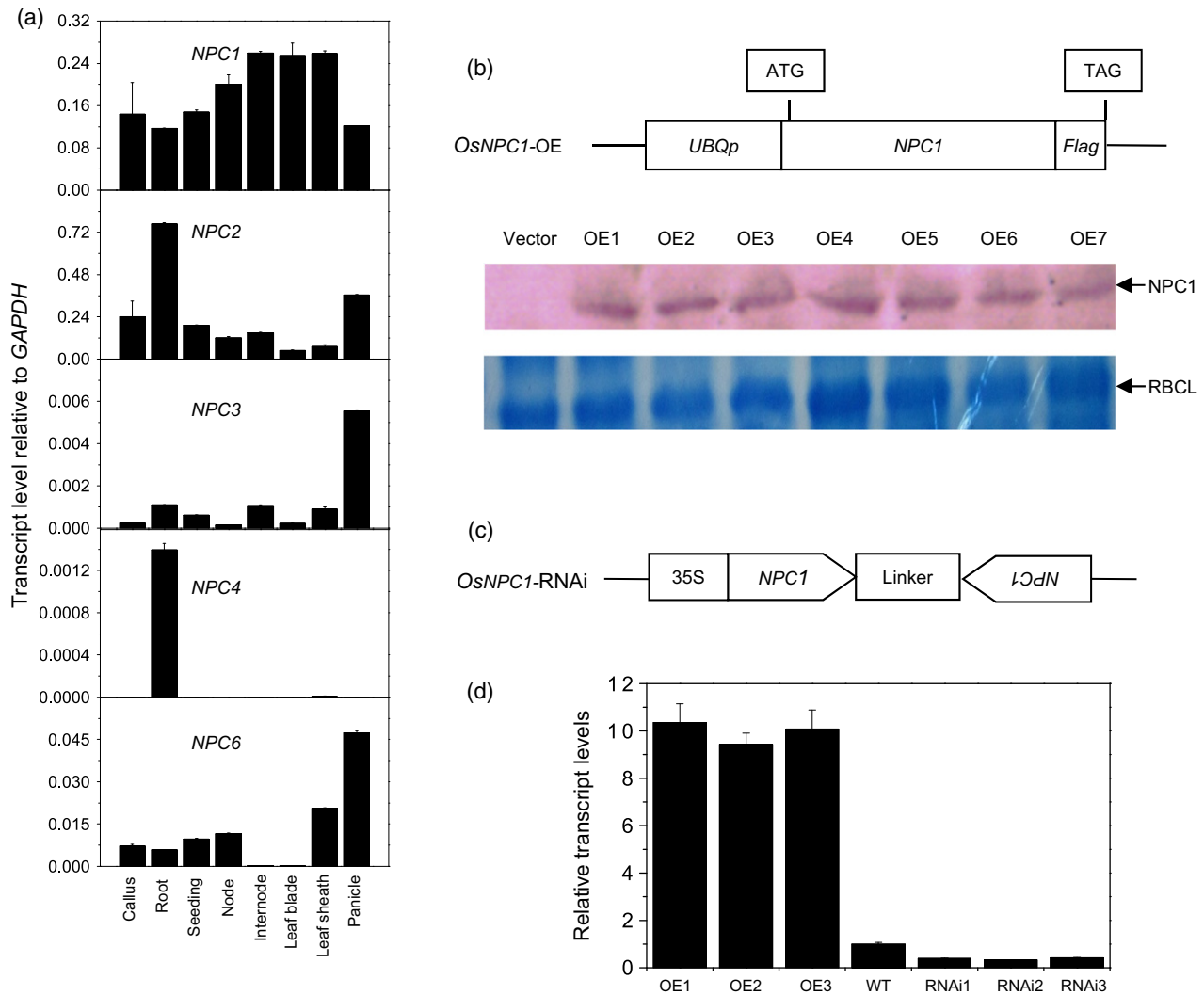


**Figure 1.** *NPC1* expression patterns and manipulation of its expression in rice. (a) Transcript level of *NPCs* in different rice tissues. RNA for seedlings, leaf blades, and leaf sheathes was extracted from rice plants at the four-leaf stage. RNA for nodes, internodes, and panicles was extracted from rice plants at flowering stage. mRNA levels of *NPCs* were quantified by real-time PCR and normalized to that of *GAPDH*. Values are means  $\pm$  standard deviation (SD) ( $n = 3$ ). (b) *NPC1*:FLAG construct (upper panel) and immunoblotting detection of the *NPC1*:FLAG protein from rice (middle panel). Leaf proteins extracted from *NPC1*:FLAG transgenic rice plants were separated by 8% SDS-PAGE, transferred to a membrane, immunoblotted with anti-FLAG antibodies, and visualized with alkaline phosphatase conjugated to a secondary anti-rabbit antibody. Lane 1 is protein from rice plants transformed with empty vector. Lanes 2 through 8 are different *NPC1*:FLAG transgenic lines, for each sample, 20  $\mu$ g total protein was loaded. Lower panel, Coomassie blue staining of a gel and the marked band corresponds to the large subunit of ribulose-1,5-bisphosphate carboxylase (RBCL). (c) Schematic diagram of the *NPC1*-RNAi construct. (d) *NPC1* transcript level in wild-type, *NPC1*-RNAi, and *NPC1*-OE lines. RNA was extracted from rice leaves. The expression levels were normalized to that of *GAPDH*. Values are means  $\pm$  standard deviation (SD) ( $n = 3$ ).

of sclerenchyma cells in *NPC1*-OE nodes was decreased by 50%, whereas that in RNAi plants increased by about 20% (Figure 3a, b). The same trend has been found in the vascular bundle fibre cells, but no significantly difference of cell length and cell width in these cells was observed among *NPC1*-OE, WT, and RNAi plants (Figure 3a, b). Results from the scanning electron microscopy also confirmed the decrease in cell wall thickness of sclerenchyma in *NPC1*-OE nodes (Figure S3a). By comparison, no

significant difference in cell wall thickness was observed for internode sclerenchyma cells among OE, WT, and RNAi plants (Figure S3b, c).

The reduction of mechanical strength in plant body may be caused by the alteration of cell wall structure (Li *et al.*, 2003). We measured the level of cellulose, hemicellulose and lignin contents in nodes and internodes of WT and *NPC1*-altered plants. Compared to WT, the level of cellulose in *NPC1*-OE nodes was decreased by approximately

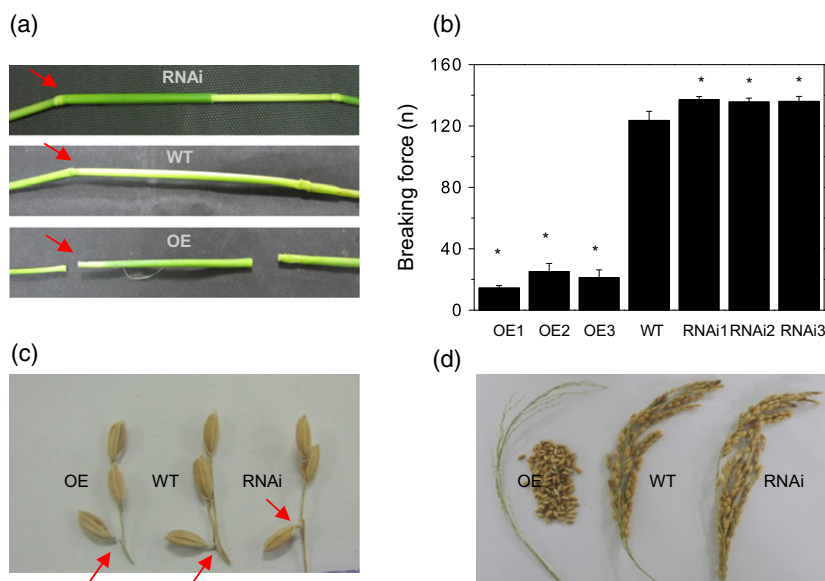
**Figure 2.** Mechanical strength and seed shattering in wide-type, *NPC1*-OE and RNAi plants.

(a) Stem breaking at the nodes by bending. Arrows indicate stem nodes.

(b) Breaking force required for stem nodes. Data are means  $\pm$  standard error (SE) ( $n = 20$ ). Asterisk indicates significant difference at  $P < 0.05$  compared with wild-type based on Student's *t*-test.

(c) Panicle node breakage. Arrows indicate the panicle nodes after hand-bending.

(d) Seed shattering of *NPC1*-OE rice. The mature seeds of *NPC1*-OE rice were easily to thresh off the head at panicle nodes.



30%, whereas that in *NPC1*-RNAi node was increased by 7% (Figure 4a, b). The level of hemicellulose in *NPC1*-OE was also decreased by about 20% (Figure 4c), but the lignin content was not altered (Figure 4d, e). By comparison, no differences of cellulose and hemicellulose content in internodes were found between WT and OE plants (Figure 4b, c). This difference is consistent with that in mechanical strength in nodes and internodes between WT and *NPC1*-altered plants, indicating that *NPC1* affects the mechanical strength and cell wall formation in nodes but not internodes.

#### ***NPC1*-OE and RNAi show opposite effects of on silicon levels in nodes and husks**

We further measured the silicon (Si) distribution in nodes and internodes because Si is a main component of the secondary cell wall in rice, and Si deficiency decreases the formation of the secondary cell wall (Blackman, 1969; Neumann *et al.*, 1999). Compared to WT plants, Si content was decreased by 25% in nodes of *NPC1*-OE rice, but increased by 10% in nodes of RNAi rice (Figure 5a). In contrast, Si content in internodes was similar among WT, OE and RNAi plants. On the other hand, Si content in husks exhibited an opposite change to that in nodes. Compared to WT plants, Si content in husks was increased by 16% in *NPC1*-OE rice but decreased by 8% in *NPC1*-RNAi plants (Figure 5b).

The opposite changes in Si content between nodes and husks might indicate an alteration of Si transport processes. We reasoned that genes that were specifically expressed in nodes and involved in Si transport and accumulation might be affected by the altered *NPC1* expression. Three proteins play important roles in Si transport in rice: *Lsi1* (Low silicon rice 1), a subgroup of

aquaporin-like proteins, is an influx transporter of silicic acid (Ma, 2004b; Ma and Yamaji, 2006; Ma *et al.*, 2007a), whereas *Lsi2* is an efflux transporter (Ma and Yamaji, 2006; Ma *et al.*, 2007a). *Lsi6* is involved in transporting silicic acid between different vascular bundles, thereby affecting silica distribution in rice above ground tissues (Yamaji *et al.*, 2008; Yamaji and Ma, 2009). Searching different databases identified that *Lsi6* was expressed in the highest levels in nodes among various rice tissues (Yamaji and Ma, 2009). We quantitatively analyzed the transcript level of *Lsi6* in different tissues and the highest level of *Lsi6* expression was detected in nodes (Figure 5c). In addition, the transcript level of *Lsi6* in *NPC1*-OE nodes was about 30% higher than that of WT and *NPC1*-RNAi nodes (Figure 5d).

#### **PA interacts with *Lsi6* and enhances the *Lsi6* and silica binding**

To test if and how *NPC1* and *Lsi6* might affect one another to impact Si distribution, potential interactions between *Lsi6* and *NPC1* were tested using a yeast two-hybrid analysis, but no direct interaction was found. We then tested the direct interaction between *Lsi6* and *NPC1*-derived lipid products, DAG and PA. *Lsi6* protein was produced and purified from *E. coli* (Figure 6a). The isolated *Lsi6* was tested for binding to various lipids. Using the same amount of *Lsi6* proteins, *Lsi6* displayed binding to PA, but not DAG, whereas control pET28 protein gave no signal on a lipid-protein blotting assay (Figure 6b). 16:0/18:1 PA and 18:1/18:1 PA displayed strong binding, but no signal was detected with di18:0 PA. This result indicates that *Lsi6* binds PA species differentially (Figure 6b). A weak signal was detectable for phosphatidylserine (PS) or PC, but no signal was detected for phosphatidylethanolamine (PE),

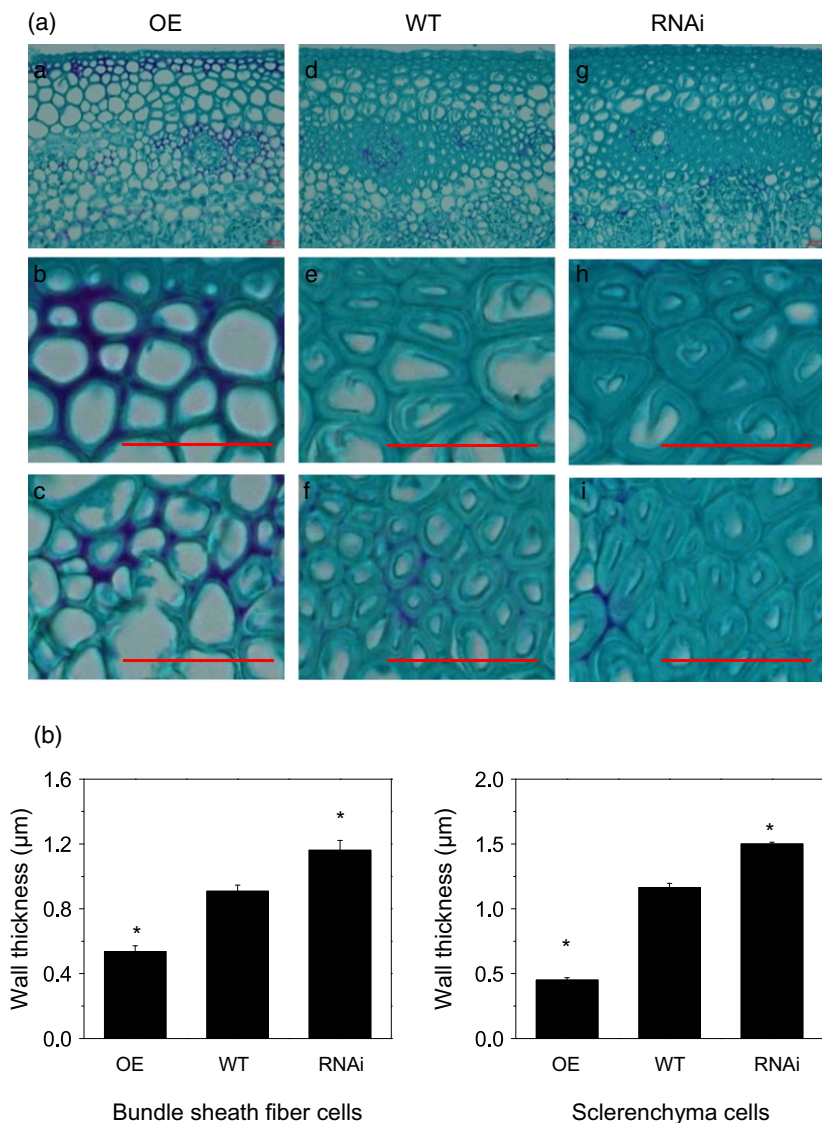


**Figure 3.** Cell morphology of node cells. (a) Cross-sections of nodes of *NPC1*-OE (a–c), wild-type (d–f), and RNAi (g–i). Scale bars = 10 µm. (b) Cell wall thickness of sclerenchyma and bundle fibre cells among the wild-type, OE and RNAi plants. Four different fields of the microscope were selected to measure the thickness of the cell wall. Data are means ± standard error (SE) ( $n = 10$ ). Asterisk indicates significant difference at  $P < 0.05$  compared with the wild-type based on Student's  $t$ -test.

phosphatidylglycerol (PG), or phosphatidylinositol (PI) (Figure 8b).

A liposome binding assay was performed to validate the interaction between PA and Lsi6, with liposomes consisting of PC only or a mixture of PC:PA (3:1 molar ratio). Liposome with PC alone failed to bind to Lsi6, whereas the binding signal was detected between PA-containing liposome and Lsi6. In addition, with the increasing amount of liposomes, Lsi6 co-pulled down with liposomes increased (Figure 6c).

In addition, the interaction between PA and Lsi6 was measured using surface plasmon resonance (SPR). The representative sensorgram shows an obviously increasing trend when the liposomes composed of PA and PC in a molar ratio of 1:3 bound to Lsi6, whereas the increase in Response Units (RUs) was much smaller when PC, PG, or PS only liposomes were used (Figure 8d). Association ( $k_a$ )

and dissociation ( $k_d$ ) constants for PA were  $172 \text{ m}^{-1} \text{ sec}^{-1}$  and  $5.47 \times 10^{-5} \text{ sec}^{-1}$ , respectively, with a binding affinity ( $KD = k_d/k_a$ ) at  $3.2 \times 10^{-7} \text{ M}$ . For PS,  $k_a$  was  $133 \text{ m}^{-1} \text{ sec}^{-1}$  and  $k_d$  was  $3.41 \times 10^{-4} \text{ sec}^{-1}$ , resulting in a  $KD$  of  $2.6 \times 10^{-6} \text{ M}$ . Thus, the binding affinity of Lsi6 to PA is more than 10 times greater than that to PS. The results above indicate that Lsi6 binds to PA with a high affinity.

Furthermore, to gain insights into the role of PA on Lsi6 function, we measured the effect of PA on Lsi6 binding to Si, using a binding assay described previously (Kröger *et al.*, 1999, 2001). Compared to the vector control protein, the amount of silicon bound to Lsi6 increased with the increased amount of the Lsi6 protein (Figure 6e). The presence of PA increased the amount of Si bound to Lsi6 (Figure 6e). At 5–10 µg protein levels, Lsi6 bound approximately 50% more Si in the presence of PA than that without PA.

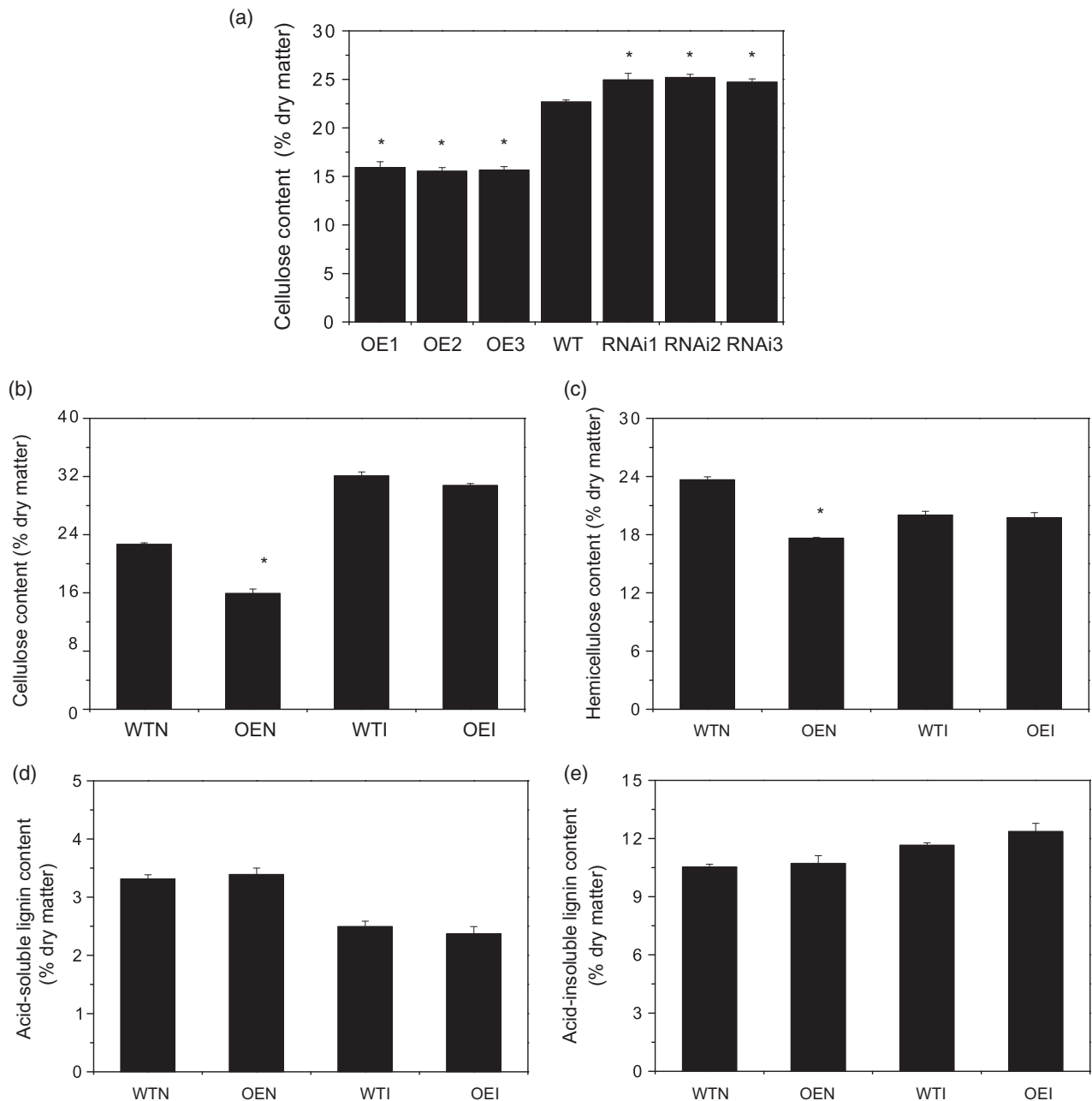


**Figure 4.** Cellulose, hemicellulose and lignin levels of wild-type and *NPC1*-altered rice.

(a) Cellulose content in rice nodes of wild-type, OE, and RNAi plants.

(b) Cellulose content in nodes and internodes of wild-type and *NPC1*-OE.

(c) Hemicellulose content in node and internodes of wild-type and OE plants.

(d) Acid-soluble lignin content in nodes and internodes of wild-type and OE plants.

(e) Acid-insoluble lignin content in nodes and internodes of wild-type and OE plants. WT and OE1 internodes and nodes were used for measurement.

WTN, Wild-type nodes sample; OEN and OEI denote nodes and internodes, respectively, of *NPC1*-OE1; WTN and WTI denote nodes and internodes, respectively, of wild-type rice plants. The samples used for content analysis were collected in the ripening stage. Data are means  $\pm$  standard error (SE) ( $n = 10$ ). Asterisk indicates significant difference at  $P < 0.05$  from wild-type based on Student's *t*-test.

#### ***NPC1* alterations affect glycerolipid composition more in nodes than internodes**

Lipid analysis of rice showed that DGDG and PA in nodes displayed opposite changes between *NPC1*-OE and RNAi

plants compared to WT (Figure 7). Whereas the level (mol %) of DGDG was lower in OE but higher in RNAi, that of PA was higher in OE but lower in RNAi plants. In addition, the level of PG, PI, and PS, was increased in *NPC1*-OE

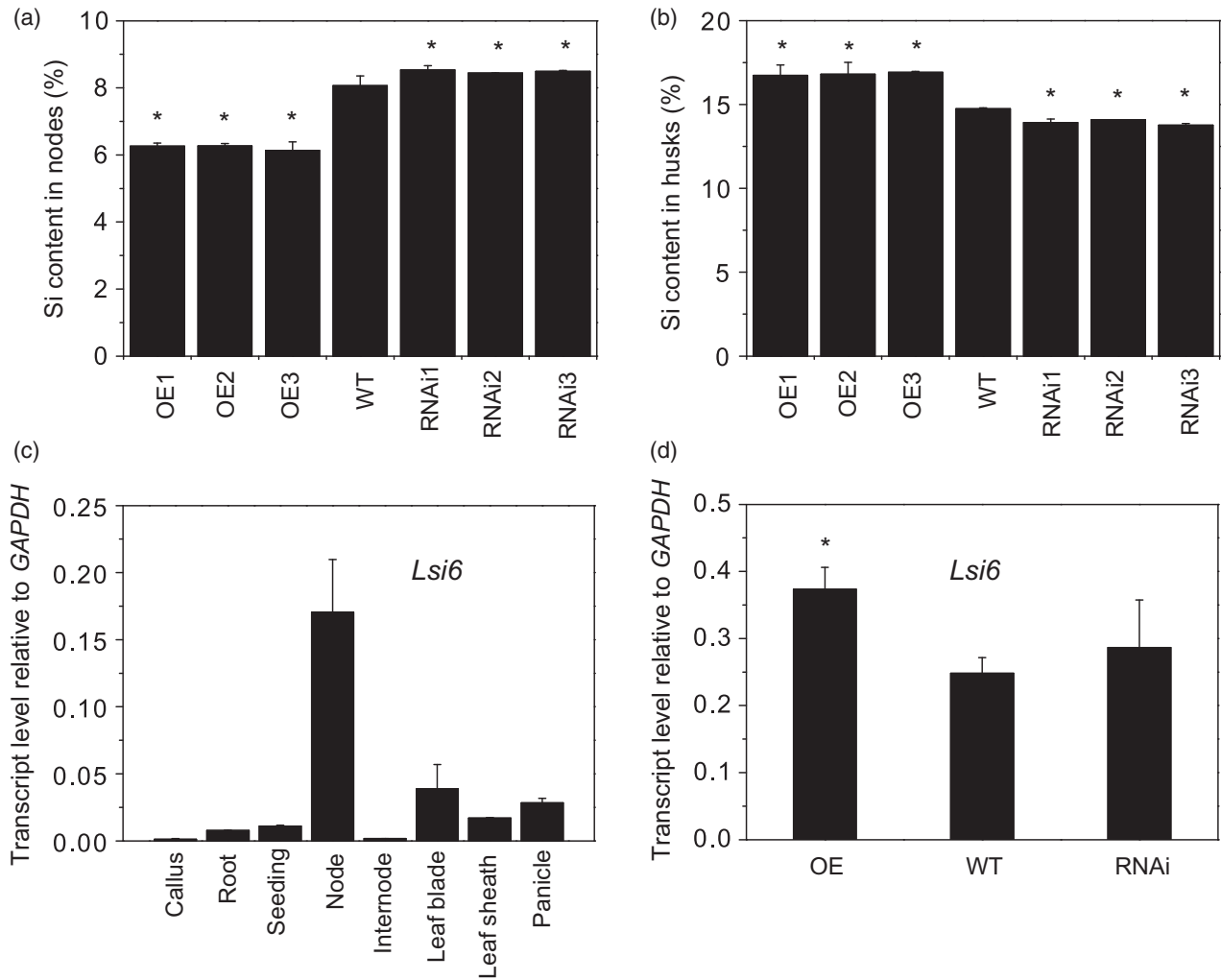


**Figure 5.** Silicon content in the nodes and husks of *NPC1*-altered and wild-type rice.

(a) Silicon content in nodes.

(b) Silicon content in husks.

(c) Transcript level of *Lsi6* in various rice tissues, as quantified by real-time PCR normalized to *GAPDH*.

(d) Transcript level of *Lsi6* in wild-type, *NPC1*-OE, and *NPC1*-RNAi rice nodes, as quantified by real-time PCR are normalized to *GAPDH*. Values in (a) and (b) are means  $\pm$  standard error (SE) ( $n = 15$ ). Asterisk indicates significant difference at  $P < 0.05$  compared with the wild-type based on Student's *t*-test. Values in (c) and (d) are means  $\pm$  standard deviation (SD) ( $n = 3$ ).

comparing to WT, whereas the level of PE, MGDG, and DGDG was decreased (Figure 7a). By comparison, except for a decrease in PA content in *NPC1*-OE plants, no significant change in lipids was found in internodes in *NPC1*-OE or RNAi rice plants (Figure 7b). The results show that *NPC1* alterations affect lipid compositions more in nodes than internodes.

To test the hydrolytic activity, we isolated NPC1: FLAG from rice leaves by immunoaffinity purification with FLAG antibodies, followed by assaying its activity. According to the assay condition previously reported for Arabidopsis NPC4 (Nakamura *et al.*, 2005; Peters *et al.*, 2010), NPC1 hydrolyzed PC, PA, PE, and PG with the highest activity toward PC (Figure 8a). NPC1 also displayed activity

towards galactolipids MGDG and DGDG, and its activity toward MGDG was about half of that toward DGDG (Figure 8a). Under the assay condition tested, NPC1 displayed comparable specific activity toward PC and DGDG. As a control, protein extracts from empty-vector-transformed rice leaves were immunoprecipitated and assayed for NPC activity, and the background activity was negligible (Figure 8a). The hydrolytic activity of NPC1 is independent of divalent cations as inclusion of EGTA in reactions did not inhibit the activity of NPC1 towards PC or MGDG, nor did any of the cations including  $\text{Ca}^{2+}$ ,  $\text{Zn}^{2+}$ ,  $\text{Mg}^{2+}$ , or  $\text{Mn}^{2+}$  increased NPC1 activity. In contrast,  $\text{Mn}^{2+}$  at the concentration tested decreased OsNPC1 activity on PC and MGDG (Figure 8b). The hydrolyzing activity of NPC1 was higher at

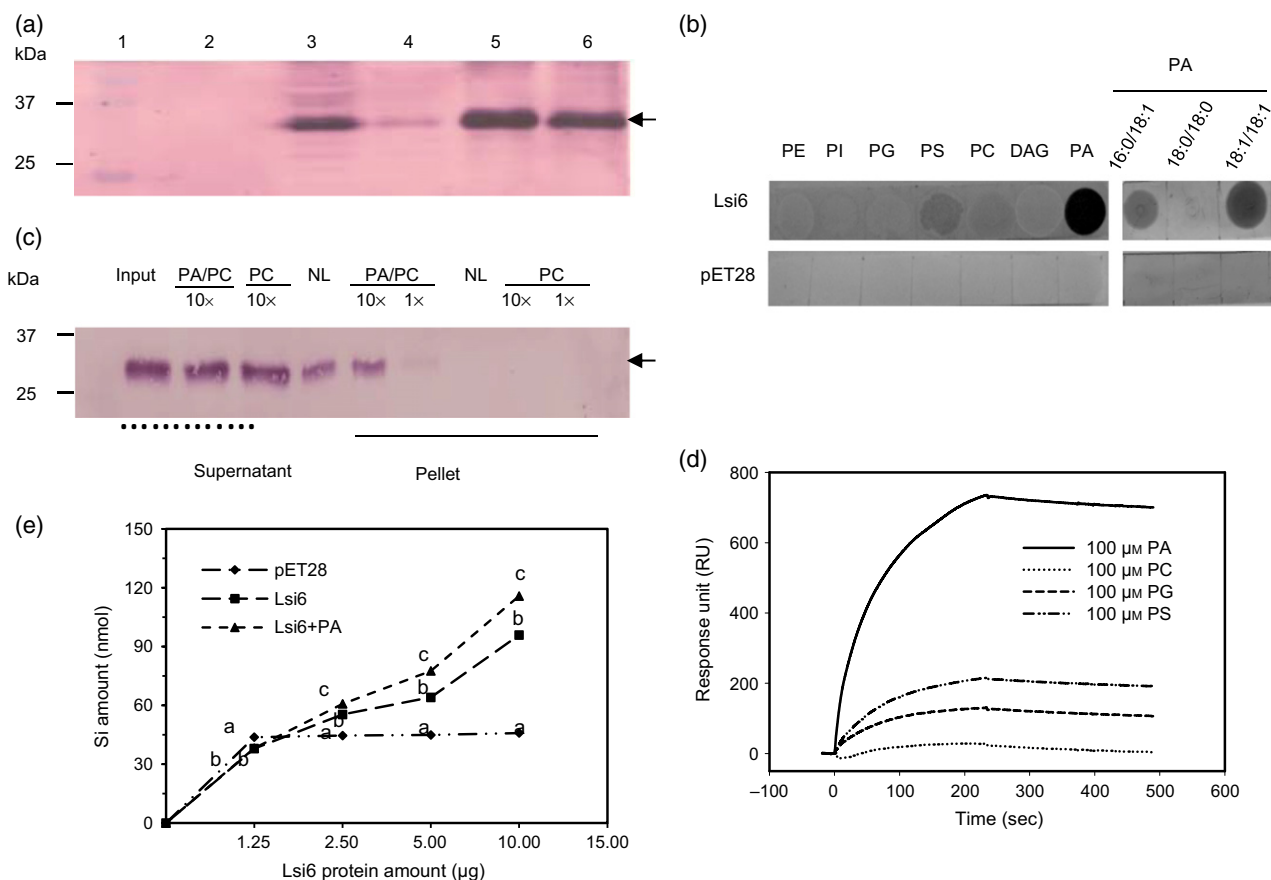


**Figure 6.** PA interaction with Lsi6.

(a) Immunoblotting of Lsi6 protein produced in *E. coli*. Lsi6 from total *E. coli* lysate was purified and separated on 12% SDS-PAGE and transferred onto a filter and blotted with anti-His antibody. 1, marker; 2, total lysate from empty vector; 3, total lysate harboring Lsi6; 4, 20 mM imidazole washing; 5, Lsi6 eluted from beads with 200 mM imidazole; 6, Lsi6 elute dialyzed with 1× PBS pH 8.0. The arrow marks Lsi6 at 31 kDa.

(b) Lipid-protein blotting of various lipids with Lsi6. 0.5  $\mu\text{g}$  of each lipid was spotted on nitrocellulose strips. PA, PC, PE and PG from chicken egg; PI from soybean; PS from porcine brain; 16:0–18:1 DAG was synthetic. The synthetic PA with defined acyl species was as specified. All the lipids are purchased from Avanti Polar Lipids.

(c) Liposomes were made up of di18:1-PC only or di18:1-PA/PC in 1/3 mole ratio. 1× and 10× refer to the concentration of PC or PA/PC liposomes used, with 10× indicating a 10 times higher concentration than 1×. NL, no liposome was used and only 25% of input Lsi6 used for liposomal binding was loaded.

(d) Representative SPR sensorgram of PA binding to Lsi6. His-Lsi6 was immobilized on the NTA chip and liposomes made of PC, PG, or PS only, or PA/PC (1/3 mole ratio) were injected. Each binding assay was repeated three times.

(e) PA effect on Si binding to Lsi6. Values are means  $\pm$  standard deviation (SD) ( $n = 4$ ). Bars with different letters denote significant difference at  $P < 0.05$ , based on analysis of variance (ANOVA) analysis and Duncan's multiple range test.

pH 5–6 than pH 8–9 (Figure 8b), indicating that NPC1 has a pH optimum at an acidic pH.

## DISCUSSION

Silicon is found in almost all plants, but its content in different plant species varies from 0.1% (low Si plants) to 10% (high Si plants) of above-ground dry weight (Epstein, 1999; Ma and Takahashi, 2002). Silicon is regarded as a 'quasi-essential element' in plant growth and development (Epstein and Bloom, 2005). Rice, a high silicon plant, can accumulate silicon as high as 10% of shoot dry weight. The level of Si increases from bottom to top tissues, such as root < stem < leaf sheath < leaf blade < husk (Ma and Takahashi, 2002). Silicon greatly enhances rice resistance

to various diseases and also alleviates adverse effects of drought and nutrient imbalance stresses (Epstein, 1999; Ma, 2004a; Ma and Yamaji, 2006). Silicon is a significant component of rice secondary cell wall, and its deficiency decreased secondary cell wall formation and reduces the mechanical strength of rice (Blackman, 1969; Neumann *et al.*, 1999). The present study indicates that NPC1 is involved in Si distribution in nodes and increased NPC1 expression decreases node Si content.

Whereas the Si content was decreased in nodes, it was increased in husks in NPC1-OE plants. This effect of NPC1-OE on Si distribution is opposite to that of Lsi6-deficient mutant in rice, in which less Si was accumulated in husks (Yamaji and Ma, 2009). In Si transport from rice root to

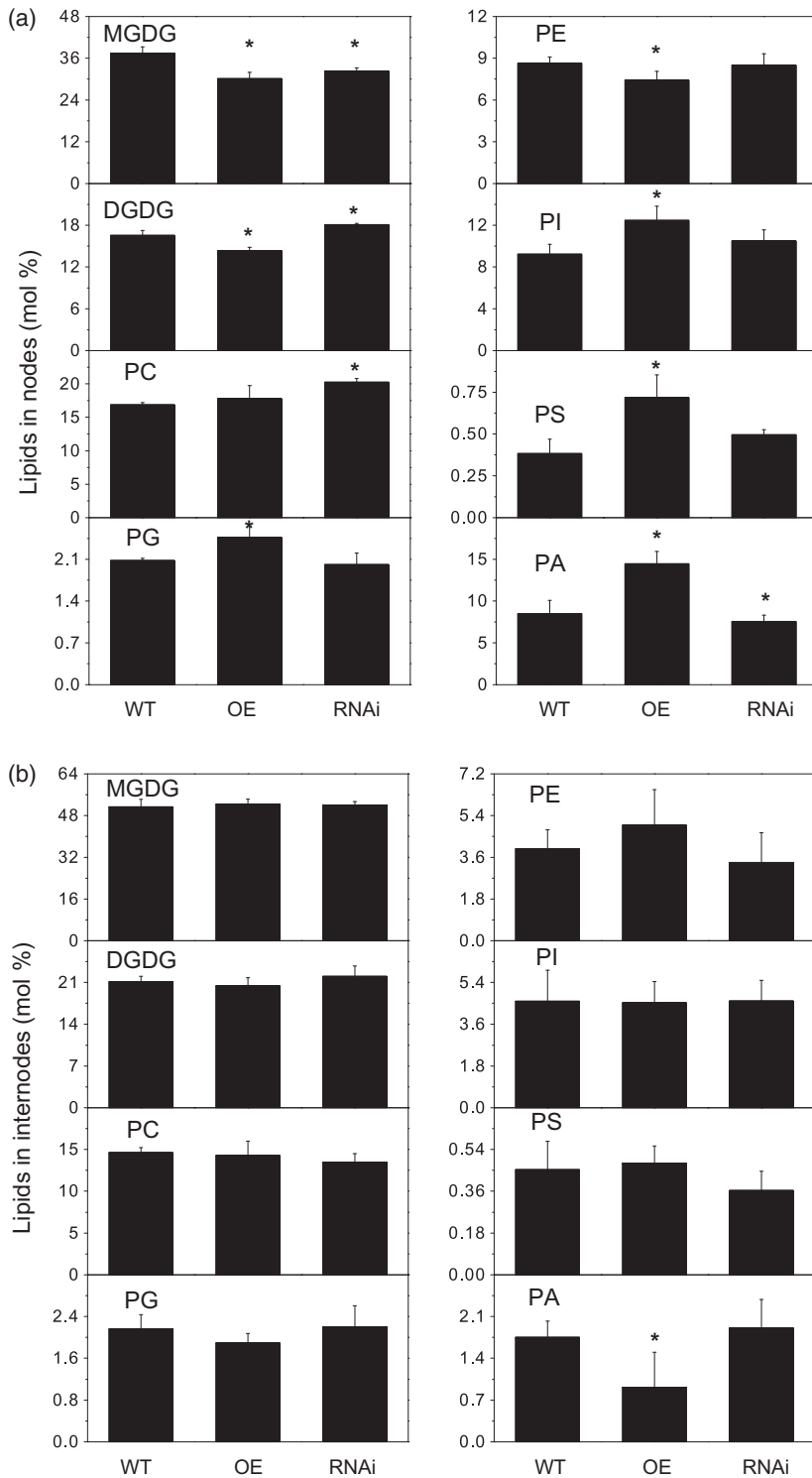


**Figure 7.** Lipid levels of wild-type, OE and RNAi in plant nodes (a) and internodes (b). Data were presented as mol% based on the total phospholipid and galactolipid content. Lipids were extracted from grain filling stage plants and analyzed by ESI-MS/MS as described by Xiao *et al.* (2010). Asterisk indicates a significant difference at  $P < 0.05$  compared with the wild-type base on Student's *t*-test. Values are means  $\pm$  standard deviation (SD) ( $n = 5$ ).

panicle, two major pathways are present in the node: One pathway is through enlarged-large vascular bundle to the flag-leaf, and the other is through diffuse vascular bundle to the panicle. A close connection exists between these two pathways and silicon can be transported from

enlarged-large vascular bundle to the diffuse vascular bundle through Lsi6 in nodes (Yamaji *et al.*, 2008; Yamaji and Ma, 2009). The present result shows that Lsi6 can bind PA, which can be derived from phosphorylation of DAG produced by NPC1 activation. This DAG to PA conversion is

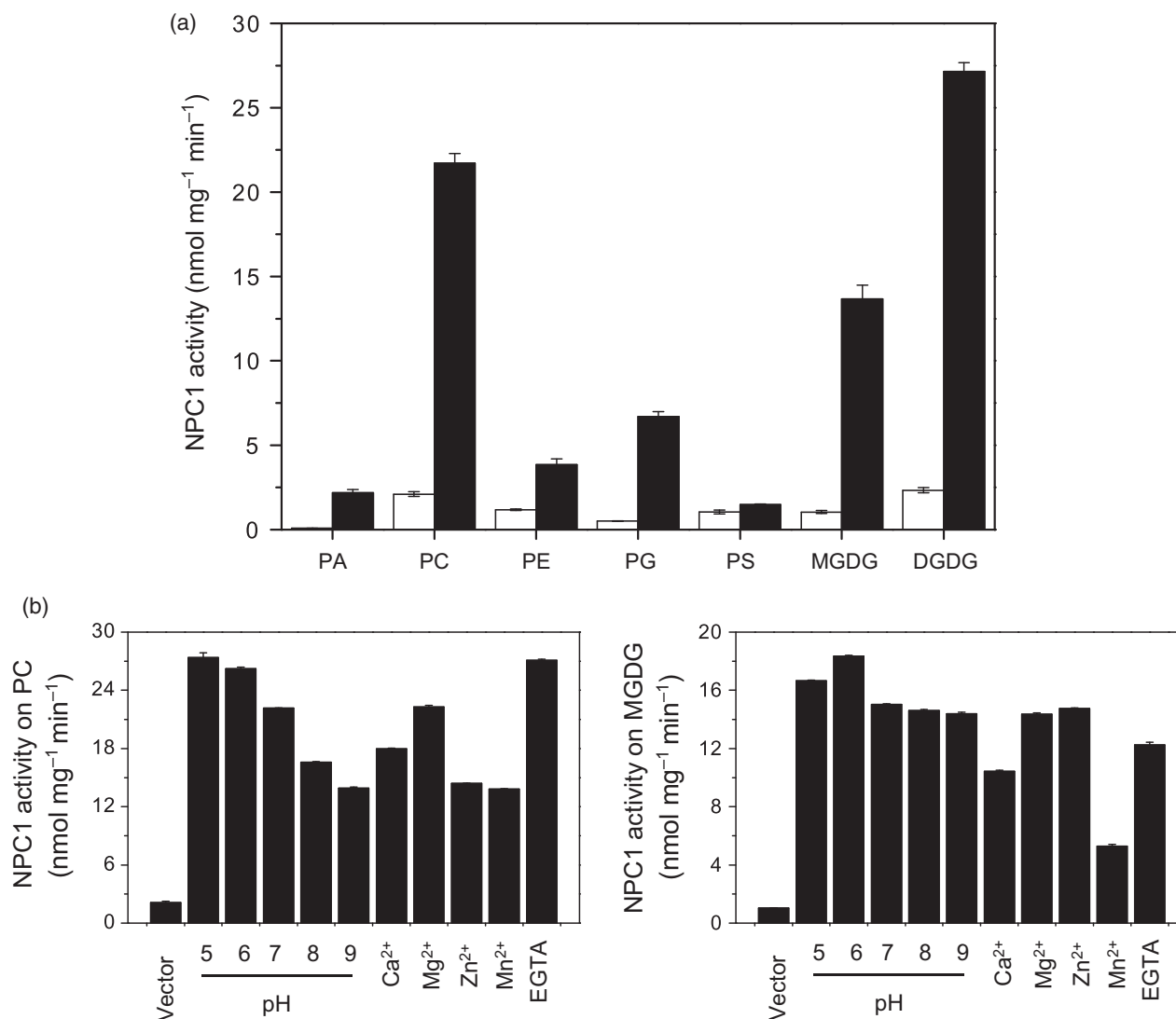


**Figure 8.** OsNPC1 activity assay *in vitro*.

(a) NPC1 hydrolysis of membrane lipids. Solid bars represented NPC1 activity from proteins immunoaffinity-purified from *OsNPC1*-FLAG rice. Open bars were activity from vector control in which the protein from rice harboring the empty vector was purified in the same manner as NPC1. Values are means  $\pm$  standard deviation (SD) ( $n = 3$ ).

(b) pH and cation effects on rice NPC1 activity towards PC and MGDG. For pH effect, no divalent ion was used, and 2 mM EGTA was used. Values are means  $\pm$  SD ( $n = 3$ ). Vector refers to the protein from rice harboring the empty vector that was purified in the same manner as NPC1.

rapid and regarded as a main mechanism of action resulting from PLC activation in plants (Arisz *et al.*, 2009). For example, PA derived from NPC4 activation plays a role in mediating root response to hyperosmotic stress (Peters *et al.*, 2010). Our result also indicates that PA enhances Lsi6 binding to Si. Therefore, it is likely that the Lsi6-PA interaction promotes Si transport cross the xylem cell membrane, thus increasing the silicon content of rice panicle tissues, such as husks.

The analysis of *NPC1*-altered rice indicates that NPC1 hinders secondary cell wall formation in nodes. The concomitant decrease in Si and cellulose in nodes raises the question of whether the decreased Si results from

decreased cellulose content/secondary cell wall formation. This is unlikely, as NPC1 is expressed in all tissues examined and not limited to cells in nodes. If the alteration of NPC1 on cellulose formation is the primary effect, one would expect that cellulose deposition would be decreased in all tissues. However, the effect is specific to cells in nodes. In addition, our data indicate that PA interacts with Lsi6 that is selectively expressed in the node. Furthermore, lipid analysis showed an increase in PA in nodes of *NPC1*-OE plants. Si deficiency is known to impede the formation of rice secondary cell wall (Blackman, 1969; Neumann *et al.*, 1999). Thus, we propose that NPC1 and its derived lipid mediator PA promotes Si transport out of nodes,

leading to a decrease in cellulose and hemicellulose production.

In addition, the enzymatic and lipid analyses provide insights into the lipid substrates for NPC1 in rice. NPC4 and NPC5 can hydrolyze different phospholipids (Nakamura *et al.*, 2005; Gaude *et al.*, 2008; Peters *et al.*, 2010, 2014). The amino acid sequences of NPC4 and NPC5 are more closely related to one another than to NPC1. A recent study found that NPC1 from *Arabidopsis* hydrolyzed PC and its activity to other lipids were not tested (Krčková *et al.*, 2015). The present results indicate that NPC1 hydrolyzes both phospholipids and galactolipids. This raises the question of what lipid substrates are for NPC1 *in vivo*. Whereas phospholipids are present in various cellular membranes, galactolipids are predominately localized in chloroplast membranes. Galactolipids, particularly DGDG, are found in outer envelope membranes of chloroplasts and even on the plasma membrane, particularly when plants are deprived of phosphorus. NPC1 has no chloroplast target signal peptide and is not present in plastids. NPC1 that is found in the cytosolic and membrane fractions may have access to galactolipids. Glycerolipid profiling of rice nodes revealed that the level of galactolipid in NPC1-OE was lower than that in WT. In contrast, the level of phospholipids in NPC1-OE was higher than that WT. Specifically, DGDG and PA levels in nodes displayed opposite changes between OE and RNAi plants compared to those of WT. The increase in phospholipid to galactolipid ratio in NPC1-OE plants appeared to be counterintuitive to the function NPC1 that was expected to hydrolyze phospholipids. The result could mean that NPC1 hydrolyzes galactolipids in plants and the overexpression of NPC1 increases galactolipid hydrolysis. DAG released by NPC1 hydrolysis could be used as substrates for phospholipid synthesis. These opposite effects of NPC1-OE and RNAi plants suggest that NPC1 is involved in homeostasis of phospholipids and galactolipids in cell membranes.

Furthermore, the current results also show that NPC1 is involved in seed shattering, which is an important agronomic trait in crop domestication and production as it can result in major crop yield loss. Several mutants affecting seed shattering have been isolated, such as *SHAT1* (*SHATTERING ABORTION1*), *SH4* (for shattering quantitative trait locus on chromosome 4), and *qSH1* (for quantitative trait locus of seed shattering on chromosome 1) (Li *et al.*, 2006; Lin *et al.*, 2007; Zhou *et al.*, 2012). The brittle panicle nodes caused easy seed shattering in NPC1-OE rice. This shattering phenotype of NPC1-OE is distinctively different from other seed shattering mutants reported previously (Zhou *et al.*, 2012). The increased expression of NPC1 decreased the mechanical strength in the panicle nodes whereas other mutants affect formation of abscission zone. In addition, the position of the break points was in the panicle nodes of NPC1-OE rice, but was in the

junction between the grain and the panicle stem for the other mutants.

Collectively, these results indicate that alteration of NPC1 expression impacts lipid levels, cellulose content, Si distribution, and mechanical strength of rice nodes. We propose that increased NPC1 expression and PA-Lsi6 interaction lead to a decreased Si content and secondary cell wall formation in nodes and an increased Si transport to and accumulation in husks. Genetic alterations of NPC1 have crucial physiological consequences to rice production as they affect stem mechanical strength and seed shattering.

## EXPERIMENTAL PROCEDURE

### Construction of NPC1 vectors and rice transformation

To overexpress NPC1, full length cDNA sequence of *OsNPC1* without the stop codon was amplified from rice Zhonghua11 (ZH11, *Oryza sativa* L. ssp. *japonica*) with the pair of primer NPC1-F/R (Table S3). The fragment was then cloned into the *KpnI* and *BamHI* sites of the overexpression vector pU1301 with a C-terminal fusion with the FLAG tag (Dai *et al.*, 2007). The expression of NPC-FLAG was under the control of the maize ubiquitin promoter. The fusion constructs were verified by DNA sequencing. The binary vectors were introduced into *Agrobacterium tumefaciens* (strain EHA105) that was used for transformation (Dai *et al.*, 2007). For knocking down the expression of NPC1, a 584-bp cDNA fragment was amplified from NPC1 cDNA with the pair of primer NPC1-RNAi-F/R (Table S3) and the resulting product was inserted into the *KpnI* and *BamHI* sites (for forward insert) and the *SacI* and *SpeI* sites (for the reverse insert) of the RNAi vector Pds1301 (Chu *et al.*, 2006). Rice Zhonghua11 was used for *Agrobacterium tumefaciens*-mediated transformation (Wu *et al.*, 2003). ZH11 seeds were surface-sterilized and germinated in dark for 45 days, and callus derived from mature embryos was used for transformation mediated by *A. tumefaciens*. Transgenic OE and RNAi rice plants were confirmed by antibiotics resistance and PCR. For OE plants, immunoblotting with the anti-FLAG antibody verified the production of NPC-FLAG protein.

### Purification of overexpressed NPC1 and assaying NPC activity

NPC1-FLAG protein was purified from NPC1-OE plant leaves with an ANTI-FLAG affinity gel (Sigma A2220; St.Louis, MO, USA) according to the manufacturer's instruction. Briefly, OE rice leaves were grinded with liquid nitrogen and homogenized in cold buffer B (50 mM Tris-HCl pH7.5, 150 mM NaCl, 50 mM sucrose, 1 mM PMSF, 0.1% Triton X-100, 1× Plant Proteinase Inhibitors). The homogenates were centrifuged at 10 000 g for 20 min. Supernatants which have been removed remaining particulates with a 0.22 μm filter were incubated with the affinity gel for 3 h with gentle agitation. The gels were washed and proteins bound to the affinity gel were competitively eluted with FLAG peptides. Protein concentration after purification was quantified by the Bradford method (Bio-Rad, Hercules, CA, USA) with bovine serum albumin (BSA) as a standard. The same immunoaffinity procedure was used to isolate the FLAG tag from the rice which was transformed with the empty vector, and such isolate was used as a negative control for the enzyme activity assay.

NPC activity was assayed using the condition previously described (Nakamura *et al.*, 2005; Peters *et al.*, 2010). The activity of NPC1 towards phospholipids (PC, PE, PS, PA, PG) and galactolipids (MGDG, DGDG) was assayed in the presence of 50 mM Tris-HCl pH 7.3, 50 mM NaCl, and 5% glycerol. DAG hydrolyzed from different lipid substrates was separated and analyzed by thin layer chromatography (TLC) and followed by GC analysis (Peters *et al.*, 2010).

### Lipid analysis

Lipid extraction and analysis were performed as described previously (Hong *et al.*, 2008). Nodes and internodes from flowing stage rice were harvested separately from same plants for lipid extraction. Extracted lipids were injected into an electrospray ionization source of a triple quadrupole mass spectrometer via continuous infusion. Phospholipids and galactolipids were quantified by comparison of peak areas to those of two internal standards of the same class (Welti, 2002; Peters *et al.*, 2010; Xiao *et al.*, 2010). The level of each lipid class was normalized to mol% of total glycerolipids analyzed. For each genotype, five independent samples were collected and analyzed separately.

### Measurements of cellulose, lignin, Si content, and mechanical strength

The content of cellulose and hemicellulose was determined on the second nodes and internodes of WT and NPC1-altered plants according to the procedure described (Xu *et al.*, 2012). A two-step acid hydrolysis procedure was used to determine the total content of lignin according to the procedure previously described (Xu *et al.*, 2012). Silicon content measurement was performed to the procedure previously reported (Yamaji *et al.*, 2008). Different rice tissues, including nodes, internodes, and husks, were harvested at the mature stage and dried at 70°C for 2 days, and then ground into powder. Solutions of 62% HNO<sub>3</sub>, 30% hydrogen peroxide and 46% hydrofluoric acid were added to each sample in a volume ratio (3: 3: 2) to a final 8 ml. After digestion, 4% boric acid was used to dilute the sample to a final 50 ml. The silicon concentration of each sample was determined according to the method previously described (Ma *et al.*, 2007b). The second nodes and internodes of rice were selected to measure the breaking force with a force testing device (DC-KZ300; Kaiming, Sichuan, China).

### Subcellular fractionation and marker enzyme assays

Leaves from 4-leaf stage NPC1-OE rice plants were homogenized were grinded in cold buffer B. The homogenates were centrifuged at 10 000 g for 20 min and the supernatant was centrifuged at 100 000 g for 60 min. The resultant supernatant was the cytosolic fraction, and the pellet as the microsomal fraction. The plasma membrane (PM) and intracellular membrane (IM) fractions were separated according to a two-phase partitioning method described previously (Fan *et al.*, 1999). The marker enzyme activities of ATPase, Cyt c reductase, and oxidase were assayed following the procedure reported earlier (Fan *et al.*, 1999).

### Microscopy imaging

Samples were prepared as reported previously (Li *et al.*, 2003). Briefly, rice node and internode tissues were excised and placed in 2.5% glutaraldehyde, followed by another fixation with 2% OsO<sub>4</sub> and then a gradient of ethanol to remove water in the sample. After that, the sample was infiltrated and embedded in butyl methyl methacrylate, then sectioned into 8 μm thick, and stained with saffron and fast green, followed by viewing under a

microscope. For scanning electron microscopy (SEM), samples were fixed in a solution with 70% ethanol, 5% acetic acid, and 3.7% formaldehyde. Samples were dehydrated and observed with a scanning electron microscope (JSM-6360; JEOL, Tokyo, Japan).

### RNA isolation and real-time PCR

Total RNA was extracted from different tissues using the Trizol reagent following the manufacturer's instruction. DNA contaminants in Total RNA was removed with DNase I digestion and a TIANscript RT Kit (Tiangen, Beijing, China) was used to synthesise the first-strand cDNA. Real-time PCR was performed with the MyiQ single-colour detection system (Bio-Rad) by monitoring the SYBR Green fluorescent. Efficiency was assessed by real-time PCR of a control gene encoding glyceraldehyde-3-phosphate dehydrogenase (*GAPDH*). The primers for different genes are listed in Table S3. The PCR conditions were: 1 cycle of 95°C for 60 sec; 45 cycles of DNA melting at 95°C for 30 sec, 55°C 30 sec for DNA annealing, and 72°C 30 sec for DNA extension; and a final extension of 72°C for 10 min.

### OsLsi6 cloning and protein production in Escherichia coli

The 0.9-kb coding sequence of *OsLsi6* was amplified by PCR using cDNA made from RNA of Zhonghua 11 at 4-leaf stage seedlings as a template and the *Lsi6*-F/R primers (Table S3). The *Lsi6* cDNA fragment was cloned into the pET28a vector that contains the 6xHis tag to the C-terminus. The *OsLsi6*-6xHis fusion construct was sequenced before it was introduced into the *E. coli* strain BL21 (DE3) for protein production. The expression of NPC1 was induced with 0.5 mM isopropyl-1-thio-β-D-galactopyranoside (IPTG) at 28°C for 2.5 h. The bacteria were then centrifuged at 10 000 g 15 min, followed by sonication in lysis (LE) buffer (50 mM NaH<sub>2</sub>PO<sub>4</sub>, pH 8.0, 300 mM NaCl, 1 mg/ml lysozyme, 5 mM DTT and 1 mM PMSF). The lysate was centrifuged at 10 000 g for 20 min and the resultant supernatant was incubated 6x His agarose beads (Novagen) for 4 h at 4°C. The beads were pelleted and washed three times with LE buffer plus 10 mM imidazole. The fusion proteins bound to agarose beads were washed with 20 volumes of LE buffer containing 10 mM imidazole. Bound protein was eluted with LE buffer containing 250 mM imidazole. NPC1 bound to the beads was eluted with LE buffer plus 250 mM imidazole. To reduce the effect of imidazole in lipid-protein interaction, the protein was dialyzed by phosphate-buffered saline, pH 8.0. The concentration of purified NPC1 protein was determined by a protein assay kit (Bio-Rad).

### Lipid-protein blotting and liposomal binding

Protein and lipid binding on filters was performed according to the procedure previously described (Stevenson *et al.*, 1998). Lipids (10 μg) were spotted on a nitrocellulose membrane and dried in the air for 1 h. The membrane with lipid was incubated with purified His-tagged protein in 1x PBST for 3–5 h in 4°C. The membrane was washed three times with 1x PBST for total 15 min, followed by incubation with the anti-His antibody conjugated with alkaline phosphatase. *Lsi6* protein that bound to lipids on membranes was visualized by staining alkaline phosphatase activity.

Liposomal binding was performed according to the procedure previously reported (Levine and Munro, 2002; Yao *et al.*, 2013). Briefly, dioleoyl PC alone or mixed with dioleoyl PA in a 3:1 molar ratio was dried under a stream of nitrogen. Lipids were rehydrated in 1 ml extrusion buffer (250 mM raffinose, 25 mM HEPES, pH 7.5, and 1 mM DTT) at 42°C for 1 h and vortexed six times for a total 2.5 min. The suspension was extruded more than 10 times

through a 0.2  $\mu\text{m}$  pore size polycarbonate membrane to produce a clear suspension liposome. The liposome suspension was diluted with three volumes binding buffer containing 25 mM HEPES, 125 mM KCl, 0.5 mM EDTA, pH 7.5, 1 mM DTT, 0.5 mM PMSF, and then centrifuged at 100 000  $g$  for 40 min. The pellet was washed three times and resuspended in 1 ml binding buffer to obtain 3.2 mM liposome. For binding assays, 100  $\mu\text{l}$  and 10  $\mu\text{l}$  liposomes were used to incubate with Lsi6 protein for 45 min at room temperature with gentle shaking. Mixture without liposome was set as a negative control. The pellet was obtained by centrifuging at 14 000  $g$  for 30 min, followed by two times washing with binding buffer. The pellet was centrifuged and resuspended with 1/10 (v/v) of 100% trichloroacetic acid, followed by washing with acetone. Proteins bound to the liposome and in the supernatants were detected by immunoblotting with a monoclonal anti-polyHis antibody conjugated with alkaline phosphatase.

### Surface plasmon resonance analysis

SPR binding assay was performed with Biacore 2000 system as described with some modifications (Yao *et al.*, 2013). His-tagged Lsi6 was purified and was dialyzed with the running buffer (0.01 M HEPES, 0.15 M NaCl, 50  $\mu\text{M}$  EDTA, pH 7.4) for 4–6 h at 4°C, and the protein concentration was determined by a protein assay kit (Bio-Rad). Biacore Sensor Chip Ni-NTA that binds His-tagged proteins was used to immobilize the proteins. For each binding assay, 500  $\mu\text{M}$  NiCl<sub>2</sub> was injected with running buffer to saturate Ni-NTA. Lsi6-His (2  $\mu\text{M}$ ) was immobilized on the sensor chip via Ni<sup>2+</sup>-NTA chelation. Di18:1 PA/di18:1 PC liposomes from a stock solution (3.2 mM) were suspended in a running buffer (0.01 M HEPES, 0.15 M NaCl, 50  $\mu\text{M}$  EDTA, pH 7.4) and injected in sequence over the surface of the sensor chip. The liposomes composed of PC, PG, or PS only were used as negative controls. The sensor chip was regenerated by stripping nickel from the surface with a regeneration buffer (0.01 M HEPES, 0.15 M NaCl, 0.35 M EDTA, pH 8.3). The sensorgrams of association and dissociation for each protein–liposome interaction were determined and plotted by Sigma Plot 10.0.

### Silica binding activity assay and silica content measurement

Lsi6-silica binding was assayed following a procedure previously described (Kröger *et al.*, 1999). Briefly, purified Lsi6 or control proteins were diluted with 100 mM sodium phosphate-citrate (pH 5.5) to a final 10  $\mu\text{l}$ . Subsequently, 3  $\mu\text{l}$  of freshly-prepared orthosilicic acid solution was added. To examine the effect of PA on Lsi6-silica binding, another 5  $\mu\text{l}$  of 10  $\mu\text{g}/\mu\text{l}$  egg yolk PA was added to a total volume of 30  $\mu\text{l}$ . Samples were centrifuged at 14 000  $g$  for 6 min, and the resultant pellet was washed four times using H<sub>2</sub>O to remove the phosphate. The pellet was resuspended in 1 M NaOH to a final volume of 10 ml, followed by incubation at 95°C for 30 min. The silicon concentration was measured with the  $\beta$ -silicomolybdate method (Iler, 1979).

### ACKNOWLEDGEMENTS

We thank Dr Yueyun Hong for suggestions and Drs Yuanyuan Tu and Ao Li (Laboratory of Biomass and Bioenergy Research Center, Huazhong Agriculture University) for the analysis of cellulose, hemicellulose, and lignin. We also thank Dr Lihong Xiong (National Key Laboratory of Crop Genetic Improvement, Huazhong Agriculture University) for providing the rice overexpression vector pU1301U and Dr. Shiping Wang (National Key Laboratory of Crop Genetic Improvement, Huazhong Agriculture University) for providing the rice RNA interference vector pds1301. The work is

supported by grants from National Natural Science Foundation of China (31470762, 31271514), the Chinese National Key Basic Research Project (2012CB114200), and the US Department of Agriculture (2016-67013-24429).

### SUPPORTING INFORMATION

Additional Supporting Information may be found in the online version of this article.

**Figure S1.** Alignment and phylogeny analysis of NPCs in plants.

**Figure S2.** NPC1 expression pattern and subcellular association in rice.

**Figure S3.** Transverse sections of nodes and internodes of WT and NPC1-altered plants.

**Table S1.** Accession number of proteins with sequence similarity to *OsNPCs*.

**Table S2.** Degree of the sequence similarity of plant *NPCs* to *OsNPC1*.

**Table S3.** Primers used for cloning and real-time PCR.

### REFERENCES

- Arisz, S.A., Testerink, C. and Munnik, T. (2009) Plant PA signaling via diacylglycerol kinase. *Biochim. Biophys. Acta*, **1791**, 869–875.
- Blackman, E. (1969) Observations on the development of the silica cells of the leaf sheath of wheat (*Triticum aestivum*). *Can. J. Bot.* **47**, 827–838.
- Chu, Z., Yuan, M., Yao, J. *et al.* (2006) Promoter mutations of an essential gene for pollen development result in disease resistance in rice. *Genes Dev.* **20**, 1250–1255.
- Dai, M., Hu, Y., Zhao, Y., Liu, H. and Zhou, D.X. (2007) A WUSCHEL-LIKE HOMEBOX gene represses a YABBY gene expression required for rice leaf development. *Plant Physiol.* **144**, 380–390.
- Epstein, E. (1999) Silicon. *Annu. Rev. Plant Physiol. Plant Mol. Biol.* **50**, 641–664.
- Epstein, E. and Bloom, A.J. (2005) *Mineral Nutrition of Plants: Principles and Perspectives*. Sunderland, MA: Sinauer Associates.
- Fan, L., Zheng, S., Cui, D. and Wang, X. (1999) Subcellular distribution and tissue expression of phospholipase D $\alpha$ , D $\beta$ , and D $\gamma$  in Arabidopsis. *Plant Physiol.* **119**, 1371–1378.
- Gaude, N., Nakamura, Y., Scheible, W.R., Ohta, H. and Dörmann, P. (2008) Phospholipase C5 (NPC5) is involved in galactolipid accumulation during phosphate limitation in leaves of Arabidopsis. *Plant J.* **56**, 28–39.
- Hong, Y., Pan, X., Welti, R. and Wang, X. (2008) Phospholipase D $\alpha$ 3 is involved in the hyperosmotic response in Arabidopsis. *Plant Cell*, **20**, 803–816.
- Iler, R. (1979) *The Chemistry of Silica*. New York: Wiley.
- Kadamur, G. and Ross, E.M. (2013) Mammalian phospholipase C. *Annu. Rev. Physiol.* **75**, 127–154.
- Kocourkova, D., Krckova, Z., Pejchar, P., Veselkova, S., Valentova, O., Wimalasekera, R., Scherer, G.F.E. and Martinec, J. (2011) The phosphatidylcholine-hydrolysing phospholipase C NPC4 plays a role in response of Arabidopsis roots to salt stress. *J. Exp. Bot.* **62**, 3753–3763.
- Krčková, Z., Brouzdová, J., Daněk, M., Kocourková, D., Rainteau, D., Rueland, E., Valentová, O., Pejchar, P. and Martinec, J. (2015) Arabidopsis non-specific phospholipase C1: characterization and its involvement in response to heat stress. *Front. Plant Sci.* **6**, 928. doi: 10.3389/fpls.
- Kröger, N., Deutzmann, R. and Sumper, M. (1999) Polycationic peptides from diatom biosilica that direct silica nanosphere formation. *Science*, **286**, 1129–1132.
- Kröger, N., Deutzmann, R. and Sumper, M. (2001) Silica-precipitating peptides from diatoms: the chemical structure of silaffin-A from *Cylindrotheca fusiformis*. *J. Biol. Chem.* **276**, 26066–26070.
- Levine, T. and Munro, S. (2002) Targeting of golgi-specific pleckstrin homology domains involves both PtdIns 4-kinase-dependent and -independent components. *Curr. Biol.* **12**, 695–704.
- Li, Y., Qian, Q., Zhou, Y. *et al.* (2003) BRITTLE CULM1, Which encodes a COBRA-like protein, affects the mechanical properties of rice plants. *Plant Cell*, **15**, 2020–2031.
- Li, C.B., Zhou, A.L. and Sang, T. (2006) Rice domestication by reducing shattering. *Science*, **311**, 1936–1939.

- Lin, Z., Griffith, M.E., Li, X., Zhu, Z., Tan, L., Fu, Y., Zhang, W., Wang, X., Xie, D. and Sun, C. (2007) Origin of seed shattering in rice (*Oryza sativa* L.). *Planta*, **226**, 11–20.
- Ma, J.F. (2004a) Role of silicon in enhancing the resistance of plants to biotic and abiotic stresses. *Soil Sci. Plant Nutr.* **50**, 11–18.
- Ma, J.F. (2004b) Characterization of the silicon uptake system and molecular mapping of the silicon transporter gene in rice. *Plant Physiol.* **136**, 3284–3289.
- Ma, J.F. and Takahashi, E. (2002) *Soil, Fertilizer, and Plant Silicon Research in Japan*. Amsterdam: Elsevier.
- Ma, J.F. and Yamaji, N. (2006) Silicon uptake and accumulation in higher plants. *Trends Plant Sci.* **11**, 392–397.
- Ma, J.F., Yamaji, N., Mitani, N., Tamai, K., Konishi, S., Fujiwara, T., Katsuhara, M. and Yano, M. (2007a) An efflux transporter of silicon in rice. *Nature*, **448**, 209–212.
- Ma, J.F., Yamaji, N., Tamai, K. and Mitani, N. (2007b) Genotypic difference in silicon uptake and expression of silicon transporter genes in rice. *Plant Physiol.* **145**, 919–924.
- Nakamura, Y., Awai, K., Masuda, T., Yoshioka, Y., Takamiya, K.I. and Ohta, H. (2005) A novel phosphatidylcholine-hydrolyzing phospholipase C induced by phosphate starvation in *Arabidopsis*. *J. Biol. Chem.* **280**, 7469–7476.
- Neumann, D., Niedem, Z. and Schwieger, W. (1999) Mechanism of heavy metal tolerance in plant. *J. Plant Physiol.* **154**, 536–546.
- Pejchar, P., Potocký, M., Novotná, Z., Veselková, Š., Kocourková, D., Valentová, O., Schwarzerová, K. and Martinec, J. (2010) Aluminium ions inhibit the formation of diacylglycerol generated by phosphatidylcholine-hydrolyzing phospholipase C in tobacco cells. *New Phytol.* **188**, 150–160.
- Pejchar, P., Potocký, M., Krčková, Z., Brouzdová, J., Danek, M. and Martinec, J. (2015) Non-specific phospholipase C4 mediates response to aluminum toxicity in *Arabidopsis thaliana*. *Front. Plant Sci.* 2015 Feb 16;6:66. doi: 10.3389/fpls.2015.00066. eCollection 2015.
- Peters, C., Li, M., Narasimhan, R., Roth, M., Welti, R. and Wang, X. (2010) Nonspecific phospholipase C NPC4 promotes responses to abscisic acid and tolerance to hyperosmotic stress in *Arabidopsis*. *Plant Cell*, **22**, 2642–2659.
- Peters, C., Kim, S.-C., Devaiah, S., Li, M. and Wang, X. (2014) Non-specific phospholipase C5 and diacylglycerol promote lateral root development under mild salt stress in *Arabidopsis*. *Plant, Cell Environ.* **37**, 2002–2013.
- Pokotylo, I., Pejchar, P., Potocký, M., Kocourková, D., Krčková, Z., Ruelland, E., Kravets, V. and Martinec, J. (2013) The plant non-specific phospholipase C gene family. Novel competitors in lipid signalling. *Prog. Lipid Res.* **52**, 62–79.
- Pokotylo, I., Kolesnikov, Y., Kravets, V., Zachowski, A. and Ruelland, E. (2014) Plant phosphoinositide-dependent phospholipases C: variations around a canonical theme. *Biochimie*, **96**, 144–157.
- Stevenson, J., Perera, I. and Boss, W. (1998) A phosphatidylinositol 4-kinase pleckstrin homology domain that binds phosphatidylinositol 4-monophosphate. *J. Biol. Chem.* **273**, 22761–22767.
- Wang, X. (2004) Lipid signaling. *Curr. Opin. Plant Biol.* **7**, 1–8.
- Welti, R. (2002) Profiling membrane lipids in plant stress responses. role of phospholipase D $\alpha$  in freezing-induced lipid changes in *Arabidopsis*. *J. Biol. Chem.* **277**, 31994–32002.
- Wimalasekera, R., Pejchar, P., Holk, A., Martinec, J. and Scherer, G.F.E. (2010) Plant phosphatidylcholine-hydrolyzing phospholipases C NPC3 and NPC4 with roles in root development and brassinolide signaling in *Arabidopsis thaliana*. *Mol. Plant*, **3**, 610–625.
- Wu, C., Li, X., Yuan, W. et al. (2003) Development of enhancer trap line for functional analysis of the rice genome. *Plant J.* **35**, 418–427.
- Xiao, S., Gao, W., Chen, Q.F., Chan, S.W., Zheng, S.X., Ma, J., Wang, M., Welti, R. and Chye, M.L. (2010) Overexpression of *Arabidopsis* Acyl-CoA binding protein ACBP3 promotes starvation-induced and age-dependent leaf senescence. *Plant Cell*, **22**, 1463–1482.
- Xu, N., Zhang, W., Ren, S. et al. (2012) Hemicelluloses negatively affect lignocellulose crystallinity for high biomass digestibility under NaOH and H<sub>2</sub>SO<sub>4</sub> pretreatments in *Miscanthus*. *Biotechnol. Biofuels*, **5**, 58.
- Yamaji, N. and Ma, J.F. (2009) A transporter at the node responsible for intervascular transfer of silicon in rice. *Plant Cell*, **21**, 2878–2883.
- Yamaji, N., Mitani, N. and Ma, J.F. (2008) A transporter regulating silicon distribution in rice shoots. *Plant Cell*, **20**, 1381–1389.
- Yao, H., Wang, G., Guo, L. and Wang, X. (2013) Phosphatidic acid interacts with a MYB transcription factor and regulates its nuclear localization and function in *Arabidopsis*. *Plant Cell*, **25**, 5030–5042.
- Zhou, Y., Li, S., Qian, Q. et al. (2009) BC10, a DUF266-containing and Golgi-located type II membrane protein, is required for cell-wall biosynthesis in rice (*Oryza sativa* L.). *Plant J.* **57**, 446–462.
- Zhou, Y., Lu, D., Li, C. et al. (2012) Genetic control of seed shattering in rice by the APETALA2 transcription factor SHATTERING ABORTION1. *Plant Cell*, **24**, 1034–1048.